A Framework of Human Impedance recognition

Jing Luo, Chao Liu, Yanan Li, Chenguang Yang

A Framework of Human impedance Estimation for Human-Robot Interaction

Jing Luo, Chao Liu, Yanan Li, Chenguang Yang*

***Abstract*—A framework for estimating the human impedance is proposed in this paper. In physical human-robot interaction (pHRI), safety and human acceptance are key issues when humans directly interact with the robots. In order to guarantee the safety and improve performance in pHRI, it is important to estimate the dynamics and intention of the human hand. In this work, we consider that a human subject physically contacts with a force sensor when a haptic device sets force in the proposed framework. The measured force, the surface electromyographic signal and the motion of the hand are used to estimate the parameters of human forearm's impedance. The effectiveness of the proposed framework is demonstrated by experimental results.**

***Index Terms*—surface electromyographic signal (sEMG), human intention, physical human-robot interaction (pHRI), impedance parameters.**

I. Introduction

Human robot interaction (HRI) is becoming an attractive topic in recent years [1] [2] [3], especially when the human and the robot perform a collaborative task in a common space [4] [5]. In this sense, safety is a key issue which is important to both the robot and human. In general, when a robot interacts a stiff environment [6] or the intention between the robot and the human is different [7] [8], the pHRI system can be unstable.

In order to guarantee the safety of HRI, the dynamics of both the robot and the human hand should be analysed. Researchers have proposed many effective robot control algorithms to achieve a safe HRI [9] [10] [11]. For example, a parameterized dynamical system was employed to allow the robots to adapt their motions to the human intention for physical HRI (pHRI) in [12]. In [13], in order to achieve seamless pHRI, a human behavior prediction method based on Gaussian Process was presented to estimate human intention.

In this paper, we concentrate on the dynamic analysis of human hand. Considering the human dynamics is closely connected to the muscle activation, we analyse the dynamics of human hand from the perspective of bioinformatics. Recently, electromyography (EMG) signals have been used to analyse the dynamics of human in pHRI. There are many achievements for analysis of human hand dynamics using EMG signals. In [14], a synchronization recognition method of gripping force and posture with respect to EMG signals was proposed to explore the relationship between EMG signal and force. An EMG-based learning method was developed to decode the grasping intention for controlling a robotic assistive device in the early stage of reach-to-grasp motion [15]. In [16], Park *et al*. proposed a motion intention decoding method based on convolutional neural network with human bio-signals. Wang *et al*. developed a teaching-learnging-prediction model to learn the human demonstrations and to predict human intention in human-robot collaborative tasks [17]. An interactive torque controller based on K-nearest neighbors algorithm by using EMG was presented for an exoskeleton robot to predict the moving direction and to change the behavior of the exoskeleton robot [18]. In [19], a multimodal framework based on EMG and mechanomyogram was developed to recognize the multi-joint motion intention of lower limb. In [20], Peternel *et al*. proposed a human-robot cooperation framework to encode the motion and impedance of human and to provide the feedback of human motor behaviour in real-time. From the above-mentioned algorithm, it can be concluded that the EMG-based method is effective to analyse the dynamics of human hand and to predict the human intention. Inspired by it, we present a neural network method to predict the interactive force between the robot and the human. Based on predicted force, we analyse the impedance parameter of human hand in the process of pHRI. The experimental results will validate the effectiveness of the proposed framework.

The rest of this paper is organized as follows. The proposed method consisting of system framework, data processing and feature selection, force prediction and impedance analysis is presented in Section II. Section III describes experimental results. Finally, conclusion of this paper is presented in Section IV.

II. Methods

A. System framework

The developed framework is presented in Fig. 1. It consists of three parts: hardware constitution, signal processing, and human intention estimation.

This work was partially supported by National Nature Science Foundation (NSFC) under Grants 61861136009 and 61811530281.

J. Luo is with the Key Laboratory of Autonomous Systems and Networked Control, College of Automation Science and Engineering, South China University of Technology, Guangzhou, 510640 China. He was also with Department of Robotics, LIRMM, UMR5506, University of Montpellier-CNRS, 161 rue Ada, 34095 Montpellier, France. (e-mail: jingluo.ac@gmail.com).

C. Liu is with Department of Robotics, LIRMM , University of Montpellier - CNRS, UMR 5506, 161 Rue Ada, 34095 Montpellier, France (e-mail: liu@lirmm.fr).

Y. Li is with the Department of Engineering and Design, University of Sussex, Brighton BN1 9RH, U.K. (e-mail: yl557@sussex.ac.uk).

C. Yang* is with Bristol Robotics Laboratory, UWE, Bristol, BS16 1QY, UK (e-mail: cyang@ieee.org).

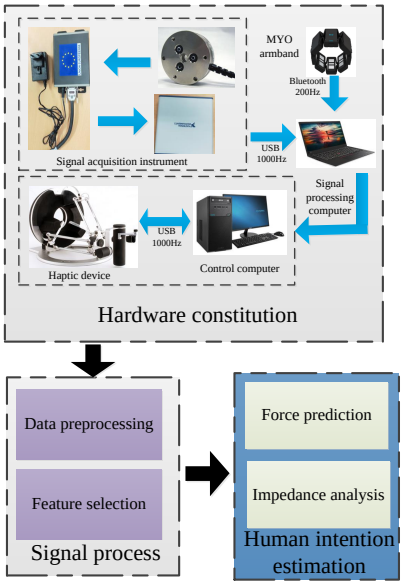

Fig. 1. The proposed system framework.

1) Hardware constitution: This part describes the system's structure which consists of signal acquisition instrument, haptic device, MYO armband, and control computer. The function of each unit is introduced in the following section and the section of experiment setup.

2) Signal Processing: This part is mainly used to process the collected interaction information such as sEMG signal, interactive force, position/velocity of the endpoint of the human hand. The data preprocessing unit is used for filtering the collected information. The feature selection unit is employed to extract the feature of the sEMG signals and to select proper features.

3) Human intention estimation: In order to estimate human intention, we predict the interactive force and use the predicted results to analyse the variation of impedance in the process of pHRI.

B. Data processing and feature selection

1) Data processing: In this section, we collect the position/velocity of the endpoint of the human hand. Because the human hand moves with the haptic device, the position/velocity can be captured by the haptic device. We collect the sEMG signals of hand by using the MYO armband. Fig. 2 shows the interactive force analysis. We have calibrated the haptic device and have compensated for the gravity of the force sensor with its appendage.

The force analysis of human robot interaction can be represented as

$$F_h = G + F_{set} \tag{1}$$

where F_{set} denotes the set force of the haptic device. G is the gravity of the force sensor with its appendage. F_h is the interactive force between the human subject and the haptic device. In this work, $G = 0\ N$ after compensating the the gravity.

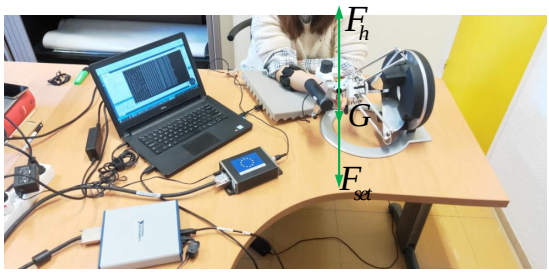

Fig. 2. Force analysis of human robot interaction.

The measured force F_h can be represented as

$$F_h = [f_x, f_y, f_z]^T \tag{2}$$

where $f_x = [f_{x1}, f_{x2}, ..., f_{xn}], f_y = [f_{y1}, f_{y2}, f_{yn}], f_z = [f_{z1}, f_{z2}, f_{zn}]$.

2) Feature selection: In order to extract the proper feature of the sEMG signals, we utilize three time domains features (RMS, AR and WL).

The RMS, AR, and WL can be represented as below

$$f_{rms} = \sqrt{\frac{1}{W_{rms}} \sum_{i=1}^{W_{rms}} n_i^2} \tag{3}$$

$$f_{wl} = \frac{1}{W_{wl}} \sum_{i=1}^{W_{wl}} \Delta n_i \tag{4}$$

$$f_{ar} = \sum_{i=1}^{p} a_i n_{k-i} + e_k \tag{5}$$

where $W_{i=rms,wl}$ represents the length of moving sampling window. n_i is the collected sEMG signal. a_i and p represent the coefficients and order of AR model, respectively. e_k represents the residual white noise.

For convenience, we utilize O_I to represent the feature of sEMG signals, which is defined as

$$O_I = [O_1, O_2, ..., O_m]^T \tag{6}$$

where $O_1 = [o_{11}, o_{12}, ..., o_{1n}], O_2 = [o_{21}, o_{22}, ..., o_{2n}], ..., O_m = [o_{m1}, o_{m2}, ..., o_{mn}]$. m is the number of input channels of sEMG signals and n is the number of sample data.

By collecting the interactive force and the feature of sEMG signals, the sample data set S_{sample} can be defined as

$$S_{sample} = [O_I, F_h]^T \tag{7}$$

C. Force prediction

In this section, we explore the relationship between the sEMG signal and the interactive force. In the stage of force prediction, we assume that there is a potential relationship of sEMG-force and the schematic diagram is presented in Fig. 3. The process of force prediction is shown in Fig. 4.

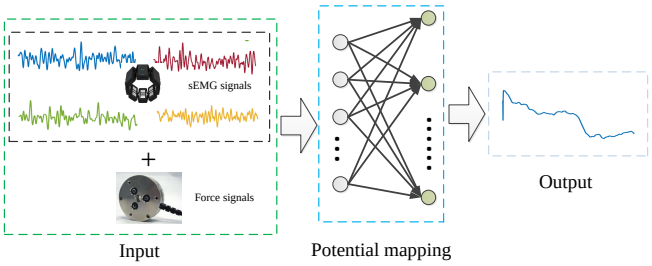

Fig. 3. Potential relationship of sEMG-force.

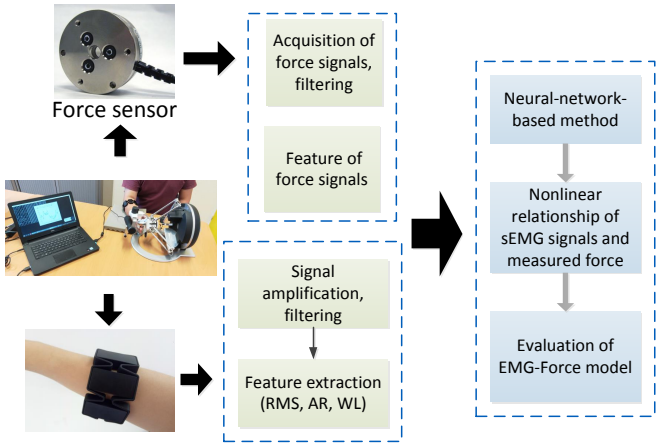

Fig. 4. The sEMG-force model by using the neural-network-based incremental learning algorithm.

Based on the above analysis, we employ a neural network method to predict the interactive force. The framework of neural network can be seen in Fig. 5.

By using the neural network method, the predicted force is presented as

$$\tilde{F} = [Z_1, ..., Z_p, H_1, ..., H_q]\ W_p^q \tag{8}$$

where $\tilde{F}$ denotes the predicted force. $Z_i, i = 1,\ 2,\ ...,\ p$ indicates the sum of feature mode. $H_i, i = 1,\ 2,\ ...,\ p$ and W_p^q are the outputs of the enhancement layer and the weight matrix, respectively.

D. Impedance analysis

The impedance of human in the HRI can be expressed as

$$F = K_D P_e + B_D \dot{P}_e + M_D \ddot{P}_e \tag{9}$$

where K_D, B_D and M_D are the stiffness matrix, the damping matrix and the inertia matrix, respectively. P_e, $\dot{P}_e$ and $\ddot{P}_e$ are the position, velocity and acceleration of human hand. Because the human hand moves with the haptic device, the position/velocity/acceleration can be captured by the haptic device.

In order to analyse the impedance of human hand, a nonlinear least squares method (LSM) is utilized in this paper.

Fig. 6 shows the process of impedance analysis, which consists of two stages: virtual impedance estimation and actual impedance estimation.

- *Virtual impedance estimation*. In this stage, we first to estimate the predicted force by using the proposed neural network method, and then employ LSM method to estimate the virtual impedance parameters based on (9).
- *Actual impedance estimation*. We can directly estimate the actual impedance parameters by collecting the measured interactive force and sEMG signals. By comparing the virtual impedance and actual impedance, we can evaluate the effectiveness of the proposed framework.

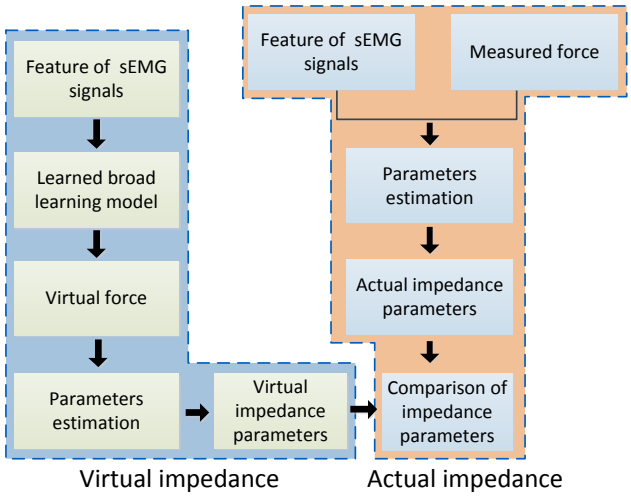

Fig. 6. The process of impedance analysis.

III. Results

A. Experimental setup

To evaluate the performance of the proposed framework, the experimental platform is configured as presented in Fig. 7.

- *Hardware equipment*. The hardware equipment contains Omega 7 (haptic device), the MYO armband, and a FT16498 force sensor.
- *Software environment*. Visual Studio 2013 and MATLAB run on the Window 7 operation system. Universal Serial Bus is used for communication between the force sensor and the control computer. The MYO armband sends the sEMG signals to the control computer by employing Bluetooth technology.

In the process of HRI, the Omega 7 can set the force according to the requirement and can capture the position, velocity and acceleration at the same time. A 3-D printed mounting is used to fix the force sensor. We have calibrated

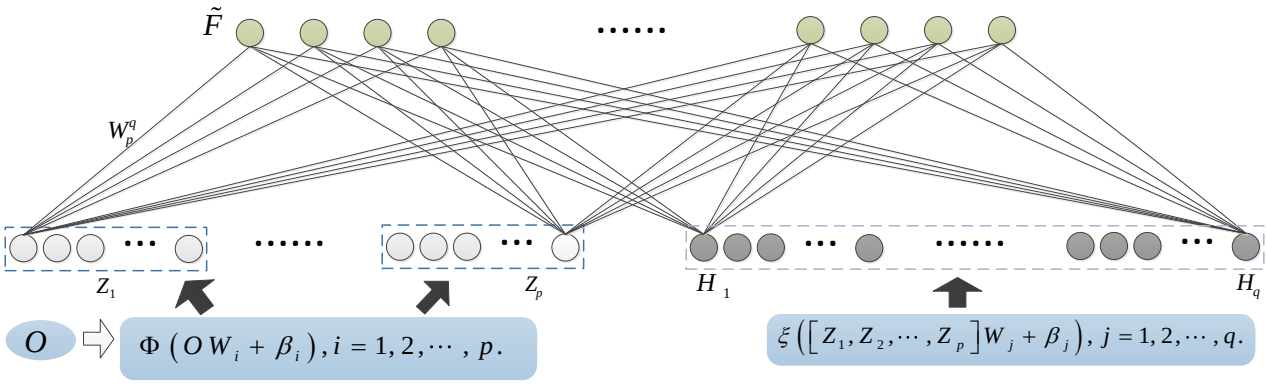

Fig. 5. Framework of force prediction algorithm. This network contains training data set (O, F_h) and p feature mappings Φ. Z_p is the sum of feature mode. ξ is the activation function. W_i is the weight matrix. O and β are the input and bias terms, respectively. $\tilde{F}$ is the output of learning algorithm, and it can be represented as $\tilde{F} = [Z_1, ..., Z_p, H_1, ..., H_q]\ W_p^q$. This algorithm needs time-consuming training to learn the neural network's parameters for learning a deep structure. Incremental learning method is used to remodel the network without a retraining process when needed to expand the neural network [21] [22] [23].

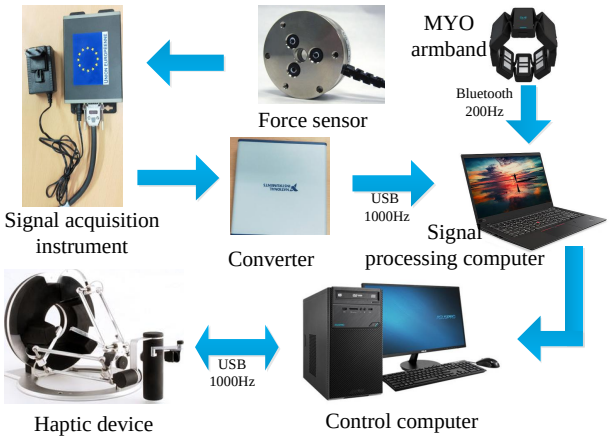

Fig. 7. The overall system.

the force sensor and the Omega 7 to compensate for the influence of its gravity. Therefore, the measured force is the interactive force.

As shown in Fig. 2, a human subject puts his finger to contact the force sensor. When we set a constant downward force for the Omega 7, human hand follows the motion of Omega 7. This system allows the hand to move in a vertical direction. In this process, we capture the sEMG signals, the interactive force and position/velocity/acceleration to estimate the impedance of hand.

B. Feature selection and force prediction

In order to properly select the sEMG feature, we utilize the RMS, AR and WL as the features to estimate the predicted force. Fig. 8 shows the RMS, AR and WL features of sEMG signals.

The predicted forces by using the proposed neural network algorithm are shown in Figs. 9-11. It can be seen that the interactive forces have been accurately predicted.

The error of predicted force by using RMS, AR and WL is presented in Fig. 12. The RMS-based performance achieves minimum error in comparison with that of AR and WL. In order to further evaluate the performance of predicted force with using different features, average error is used in this paper. From Tab. I, the average error for RMS, AR and WL are 3.3906 $\times 10^{-6}$ N, 16.453 $\times 10^{-6}$ N, and 6.6297 $\times 10^{-6}$ N, respectively.

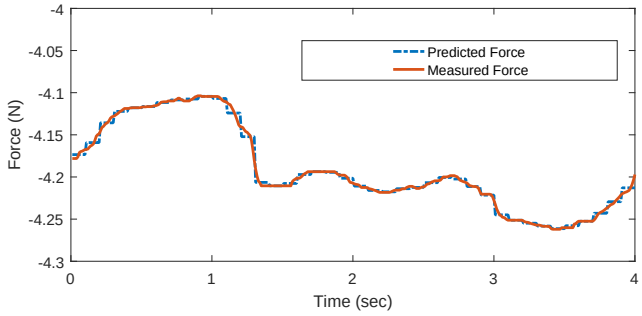

Fig. 9. Predicted force by using the proposed neural network algorithm with RMS feature.

TABLE I
AVERAGE ERROR OF FORCE PREDICTION WITH RMS, AR, AND WL FEATURES

Average error	RMS	AR	WL
Unit ($\times 10^{-6}$ N)	3.3906	16.453	6.6297

C. Stiffness analysis

In this experiment, we assume that the forces in X and Y directions are zero, so we just perform the experiment in Z-direction. In order to obtain the virtual stiffness, we first estimate the force based on the force prediction algorithm.

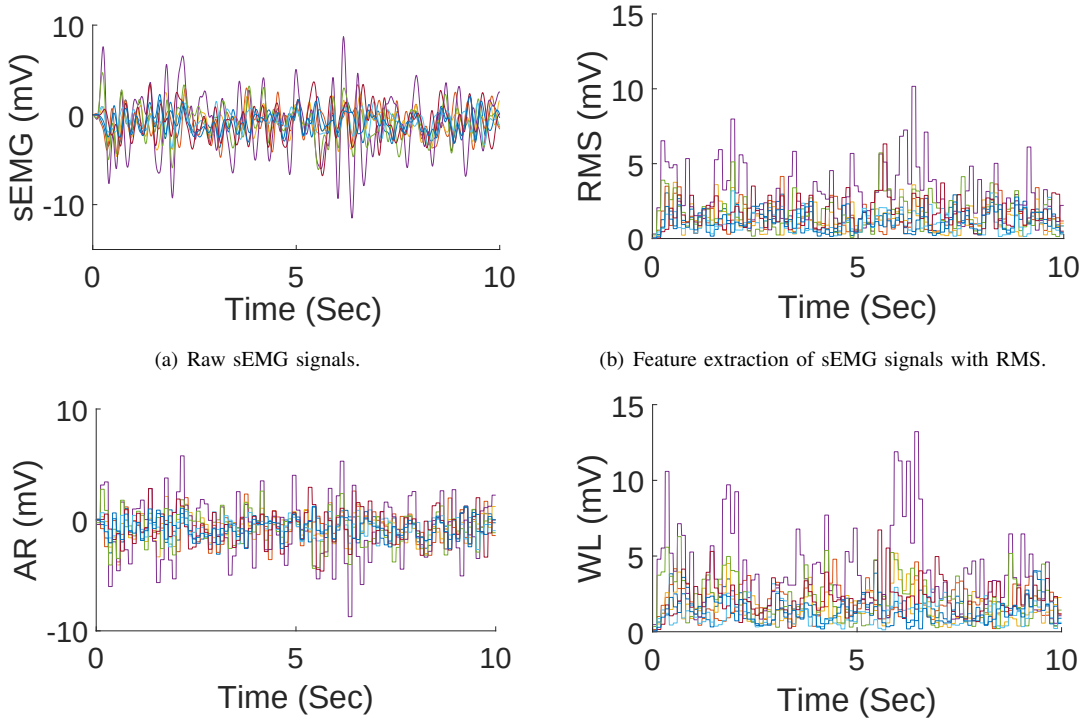

(a) Raw sEMG signals.

(b) Feature extraction of sEMG signals with RMS.

(c) Feature extraction of sEMG signals with AR.

(d) Feature extraction of sEMG signals with WL.

Fig. 8. Fig. 8(a) shows the raw sEMG signals. Fig. 8(b) shows the sEMG signals feature with RMS. Fig. 8(c) shows the sEMG signals feature with AR. Fig. 8(d) shows the sEMG signals feature with WL.

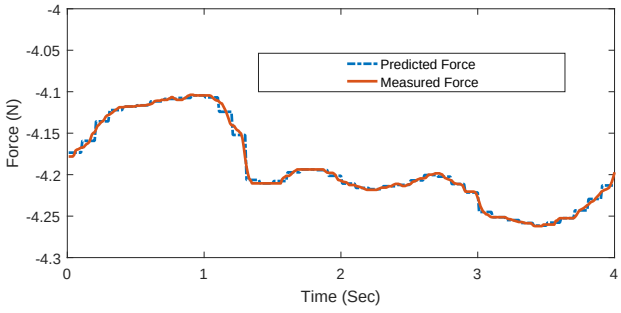

Fig. 10. Predicted force by using the proposed neural network algorithm with WL feature.

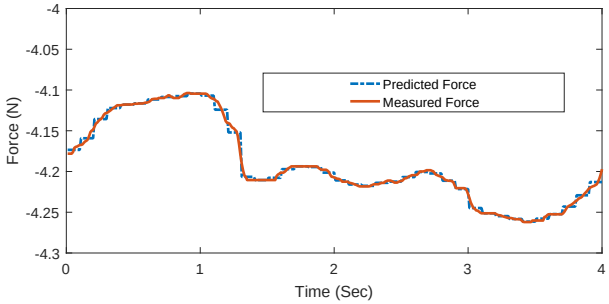

Fig. 11. Predicted force by using the proposed neural network algorithm with AR feature.

Then, the virtual stiffness can be evaluated according to the estimated force and actual position using LSM method.

From Fig. 13, it can be seen that the virtual stiffness curves almost overlap with that of actual stiffness. In Fig. 14, it can be seen that the error between virtual stiffness and actual stiffness is very small. In Table II, the values of virtual stiffness and actual stiffness are 11.0890 N/m and 11.0518 N/m, respectively. With these results, it can be concluded that the virtual stiffness can represent the actual stiffness.

TABLE II
AVERAGE STIFFNESS.

Average stiffness	Actual stiffness	Virtual stiffness
Unit (N/m)	11.0890	11.0518

IV. CONCLUSION

In this paper, we proposed a novel framework to estimate the impedance of human hand in pHRI. We utilized three features (RMS, AR and WL) to estimate the interactive force and the RMS-based prediction achieved the minimum error. According to the experimental results, the virtual impedance were in accordance with the actual impedance. In this sense, the proposed framework was effective for estimating intention of human hand.

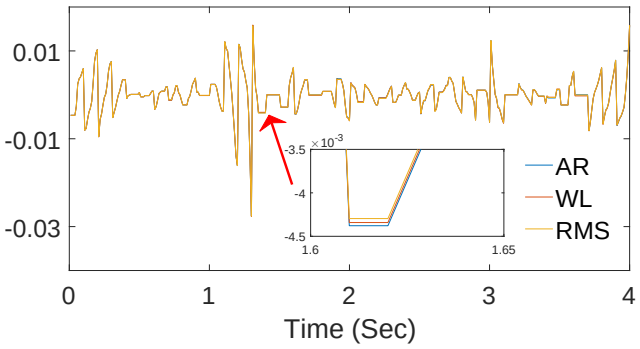

Fig. 12. Error of estimated force by using RMS, AR and WL features.

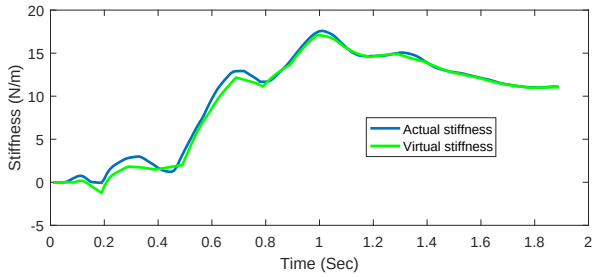

Fig. 13. Actual and virtual stiffness.

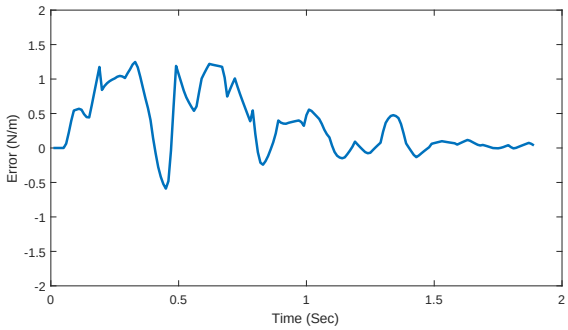

Fig. 14. Error of stiffness.

REFERENCES

[1] M. A. Goodrich, A. C. Schultz, *et al.*, "Human–robot interaction: a survey," *Foundations and Trends® in Human–Computer Interaction*, vol. 1, no. 3, pp. 203–275, 2008.

[2] T. B. Sheridan, "Human–robot interaction: status and challenges," *Human factors*, vol. 58, no. 4, pp. 525–532, 2016.

[3] J. Luo, C. Yang, Q. Li, and M. Wang, "A task learning mechanism for the telerobots," *International Journal of Humanoid Robotics*, 2019.

[4] G. Tonietti, R. Schiavi, and A. Bicchi, "Design and control of a variable stiffness actuator for safe and fast physical human/robot interaction," in *Proceedings of the 2005 IEEE international conference on robotics and automation*, pp. 526–531, IEEE, 2005.

[5] P. A. Lasota, T. Fong, J. A. Shah, *et al.*, "A survey of methods for safe human-robot interaction," *Foundations and Trends® in Robotics*, vol. 5, no. 4, pp. 261–349, 2017.

[6] F. Ficuciello, L. Villani, and B. Siciliano, "Impedance control of redundant manipulators for safe human-robot collaboration," *Acta Polytechnica Hungarica*, vol. 13, no. 1, pp. 223–238, 2016.

[7] D. Surdilovic, "Contact stability issues in position based impedance control: Theory and experiments," in *Proceedings of IEEE International Conference on Robotics and Automation*, vol. 2, pp. 1675–1680, IEEE, 1996.

[8] K. H. Lee, S. G. Baek, H. J. Lee, H. R. Choi, H. Moon, and J. C. Koo, "Improving transparency in physical human-robot interaction using an impedance compensator," in *2017 IEEE/RSJ International Conference on Intelligent Robots and Systems (IROS)*, pp. 3591–3596, IEEE, 2017.

[9] J. Luo, C. Yang, N. Wang, and M. Wang, "Enhanced teleoperation performance using hybrid control and virtual fixture," *International Journal of Systems Science*, vol. 50, no. 3, pp. 451–462, 2019.

[10] Y. Li, K. P. Tee, W. L. Chan, R. Yan, Y. Chua, and D. K. Limbu, "Continuous role adaptation for human–robot shared control," *IEEE Transactions on Robotics*, vol. 31, no. 3, pp. 672–681, 2015.

[11] W. He, Z. Li, and C. P. Chen, "A survey of human-centered intelligent robots: issues and challenges," *IEEE/CAA Journal of Automatica Sinica*, vol. 4, no. 4, pp. 602–609, 2017.

[12] M. Khoramshahi and A. Billard, "Intention-based motion adaptation using dynamical systems with human in the loop," *Power [Nm/s]*, vol. 4, no. 2, 2018.

[13] J. R. Medina, S. Endo, and S. Hirche, "Impedance-based gaussian processes for predicting human behavior during physical interaction," in *2016 IEEE International Conference on Robotics and Automation (ICRA)*, pp. 3055–3061, IEEE, 2016.

[14] J. Hua and S. Liao, "A method for synchronously predicting human intention based on posture and force," in *2018 7th International Conference on Sustainable Energy and Environment Engineering (ICSEEE 2018)*, Atlantis Press, 2018.

[15] I. Batzianoulis, S. El-Khoury, E. Pirondini, M. Coscia, S. Micera, and A. Billard, "Emg-based decoding of grasp gestures in reaching-to-grasping motions," *Robotics and Autonomous Systems*, vol. 91, pp. 59–70, 2017.

[16] K.-H. Park and S.-W. Lee, "Movement intention decoding based on deep learning for multiuser myoelectric interfaces," in *2016 4th International Winter Conference on Brain-Computer Interface (BCI)*, pp. 1–2, IEEE, 2016.

[17] W. Wang, R. Li, Y. Chen, and Y. Jia, "Human intention prediction in human-robot collaborative tasks," in *Companion of the 2018 ACM/IEEE International Conference on Human-Robot Interaction*, pp. 279–280, ACM, 2018.

[18] L.-K. Liu, L.-Y. Chien, S.-H. Pan, J.-L. Ren, C.-L. Chiao, W.-H. Chen, L.-C. Fu, and J.-S. Lai, "Interactive torque controller with electromyography intention prediction implemented on exoskeleton robot ntuh-ii," in *2017 IEEE International Conference on Robotics and Biomimetics (ROBIO)*, pp. 1485–1490, IEEE, 2017.

[19] C. Cui, G.-B. Bian, Z.-G. Hou, J. Zhao, and H. Zhou, "A multimodal framework based on integration of cortical and muscular activities for decoding human intentions about lower limb motions," *IEEE transactions on biomedical circuits and systems*, vol. 11, no. 4, pp. 889–899, 2017.

[20] L. Peternel, N. Tsagarakis, and A. Ajoudani, "Towards multi-modal intention interfaces for human-robot co-manipulation," in *2016 IEEE/RSJ international conference on intelligent robots and systems (IROS)*, pp. 2663–2669, IEEE, 2016.

[21] C. P. Chen and Z. Liu, "Broad learning system: An effective and efficient incremental learning system without the need for deep architecture," *IEEE transactions on neural networks and learning systems*, vol. 29, no. 1, pp. 10–24, 2018.

[22] C. P. Chen, Z. Liu, and S. Feng, "Universal approximation capability of broad learning system and its structural variations," *IEEE transactions on neural networks and learning systems*, no. 99, pp. 1–14, 2018.

[23] S. Feng and C. P. Chen, "Fuzzy broad learning system: a novel neuro-fuzzy model for regression and classification," *IEEE transactions on cybernetics*, no. 99, pp. 1–11, 2018.